Metalens Array for Integral-Imaging-Based Near-Eye Display

Zhi-Bin Fan[1,3], Yun-Fan Cheng[2,3,4], Xia Liu[1,3], Wen-Long Lu[1,3], Zong Qin[2,3,4] and Jian-Wen Dong[1,3]

[1]School of Physics, Sun Yat-Sen University, Guangzhou, China

[2]School of Electronics and Information Technology, Sun Yat-Sen University, Guangzhou, China

[3]State Key Laboratory of Optoelectronic Materials and Technologies, Sun Yat-Sen University, Guangzhou, China

[4]Guangdong Province Key Laboratory of Display Material and Technology, Sun Yat-Sen University, Guangzhou, China

Abstract

We propose a novel integral-imaging (II) based near-eye display (NED) combined with high-pixel-density display screen, voxel-based rendering method and nano-imprint metalens array. The effect of depth of field in AR and VR of such II-based NED is shown, and the 3D parallax effect on the real mode is demonstrated. We successfully miniaturize the II-based NED which shows a great potential using in AR and VR.

Author Keywords

Integral imaging; near-eye display; metalens array; AR; VR.

1. Introduction

Virtual reality (VR) and augmented reality (AR) near-eye display (NED) technologies are expected to subvert traditional display technologies in various information output modes, showing great application potential in exhibition, education, medical treatment, entertainment and other fields. Today's near-eye 3D display products mostly use the principle of binocular parallax to display a pair of plane images on the retina of human eyes, and promote image fusion through the brain to generate 3D perception. However, the focus depth and the convergence depth are different in such binocular parallax display [1,2], which brings the vergence accommodation conflict (VAC) problem. People will feel vertiginous when using this kind of near-eye 3D display.

Recently, researchers pay attention to 3D displays [3] without VAC problem, for example, holography display and II display [4,5]. They provide visual stimulation equivalent to that of the real world, more in line with human visual mechanism, and hence no VAC problem exists. II display usually uses the microlens array and 2D screen to reconstruct 3D images, and has the unique advantages, such as simple device, no coherent noise spots, quasi-continuous light field and small amount of data. Early on, II display was mainly used in the field of glass-free 3D display [6-8]. In recent years, II technology has also been applied to NED system to realize the VAC-free 3D NED. Various methods [9-12] have been proposed to improve the performances of II-based NED such as resolution [10], field of view [10], depth of field [11], and rendering time [12]. In particular, a novel nano component called metalens array is applied to II display as well [8], due to the flexible ability of light field manipulation. Although the depth-of-field effect has been proved in the past research on metalens, the experiment of parallax effect is still a blank. The actual effect by integrating the metalens array and the real display panel is also lack of achievement. On the other hand, it is noticed that deep ultra violet lithography technologies [13,14] have been used to realize the low-cost, large diameter and large area metalens, and the nanoimprint technologies [15-17] are also proposed to fast reproduce metalens samples in recent years. Such advances in metalens fabrication have greatly boosted the interest in the fields of metalens array-based II display [8] and metalens-based VR/AR [17-23].

Here, we make efforts in the screen, algorithm and light control elements to build a novel II-based NED architecture by the integration of micro-display and metalens array, as shown in figure 1. Firstly, our metalens array with 2mm×2mm aperture is designed and experimentally fabricated by the nanoimprint technology. Then, a fast rendering method of II-based NED is proposed to quickly generate the film sources of 3D objects. Under such method, we realize the 3D AR display on virtual mode by showing the effects of virtual 3D images fused with surrounding objects. Finally, the 3D parallax effect of II display on real mode is also validated in experiments.

2. Optical architecture of the II-based NED using metalens array

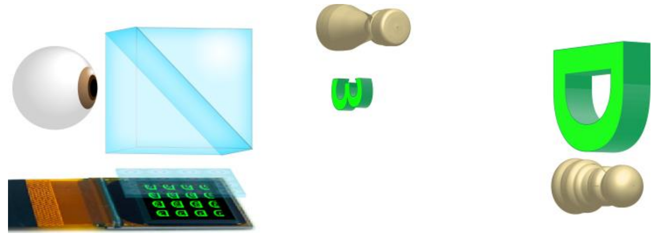

Figure 1. Schematic illustration of II-based NED with nano-imprint metalens array in AR.

The basic architecture of II-based NED with nano-imprint metalens array in AR is shown in Fig. 1. We choose the 0.39-inch micro-display of BOE, which has a high pixel density of 5644 PPI and a small pixel pitch of about 4.6 μm. In this paper, we design a virtual 3D pattern with depth-of-field effect. The reconstructed 3D images are located far behind the micro-display panel on the virtual mode, and human eye can simultaneously observe the virtual 3D pattern and the real scene (chess pieces at different depth positions) using a beam splitting prism, as the AR display effect shown in figure 1.

Figure 2 demonstrates the picture of the micro-display panel and metalens array used in this paper. In order to facilitate the assembly of the micro-display and the metalens array, we specially design a 3D-printed holder, as shown at the bottom right in figure 2. The micro-display and the metalens array can be well aligned and assembled on both sides of the holder, so as to form a convenient 3D NED module. Noted that the entire 3D NED module with the driver circuit weighs only 7.23g, facilitating the compactness on the AR systems.

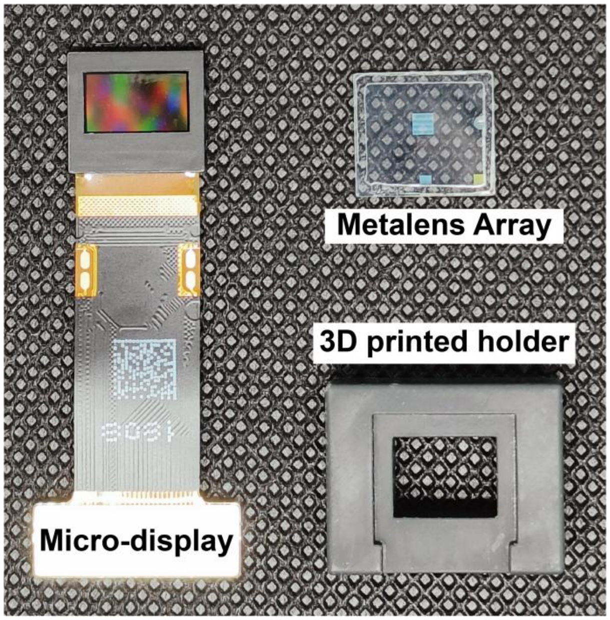

Figure 2. Components of the 3D display panel for the II-based NED, including the micro-display panel, the metalens array and the customized 3D-printed holder.

In terms of the metalens array, we combine with the metalens array obtained by nano-imprinting, which shows a great potential to ensure the quality of metalens array in large-scale production. The SEM imaging of the metalens array obtained by nano-imprinting is shown in figure 3(a), and figure 3(b) provides the top view of the local electron microscope image of the metalens array. Such array has 4×4 metalenses inside, of which the total size is 1.84 mm×1.84 mm. Figure 2(c) shows the normalized light intensity distributions of a single metalens in the array in the yz plane at 547 nm. The focal length and the focal depth are about 5.8 mm and 400 μm, respectively, and the corresponding numerical aperture of the metalens array is about 0.05. The intensity distribution in the focal plane, the intensity distribution along the x direction of a single metalens at 547 nm is shown in figure 3 (d,e). An Airy fit process of measured data is used for the calculation of the full widths at half-maximum (FWHM) in figure 3(e). The FWHM of the focal spot half-height width is 6.58 μm. We also calculate the MTF curve, getting that the cut-off frequency is about 150 lp/mm. Because the metalenses in array have the square aperture, the aperture used in the calculation of the diffraction limit is the diagonal of the metalens instead of the side length, so the actual MTF curve of the metalens is generally lower than the calculated MTF diffraction limit line. Therefore, the metalens' focusing performance is close to the diffraction-limited characteristic.

In addition, as for the film source in II display, a new fast rendering method is proposed to accelerate the elemental image array generation process and to calculate the final film source in the micro-display panel. Briefly here, we pre-calculate and store all voxel-pixel mappings to avoid massive computations in the conventional geometric projection method. Finally, the speed is improved since only the assignment is needed in the rendering step.

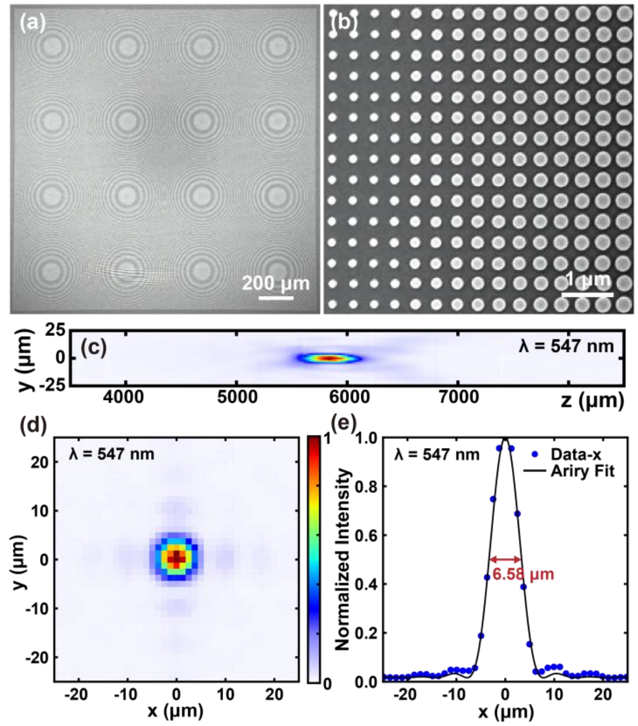

Figure 3. SEM images of metalens array and the measured results of a single metalens inside. (a) Top-view SEM image of the whole nano-imprint metalens array. Scale bar, 200 μm. (b) Top-view SEM image of a portion of the metalens array. Scale bar, 1 μm. (c) Normalized measured distribution in y-z plane at the wavelength of 547 nm. (d) Measured intensity patterns in the focal plane at 547 nm. (e)The x-direction cross section of the measured intensity profile at 547 nm. The black solid curve denotes the Airy fit of measured data (blue points). The red text gives the full widths at half-maximum of the fitting measured data.

3. Performance of II-based NED

3.1 Depth effect in AR mode

Based on the above-mentioned novel II-based NED architecture, we show the effect of depth of field in AR mode and the effect of 3D real image parallax of II. As shown in figure 1, the light of the real world enters the eye through the prism, and the light of NED is reflected into the eye by the prism, thus achieving the effect of AR. We put the chess pieces at different distances to show the relative position of the reconstructed 3D image in space. Figure 4 shows the reconstructed 3D images of II-based NED with nano-imprint metalens array in AR. When the human eye focuses on the front chess piece "Rook", the number "3" is clear and the letter "D" is blurred, illustrating that the reconstructed number "3" is at the same distance as the front chess piece "Rook". When the focus plane moves to the near chess piece "Pawn", letter "D" becomes clear and number "3" vanishes entirely. That is, the reconstructed "D" is at the same distance as the near chess piece "Pawn". The depth-of-field effect of II-based NED using metalens array has been verified.

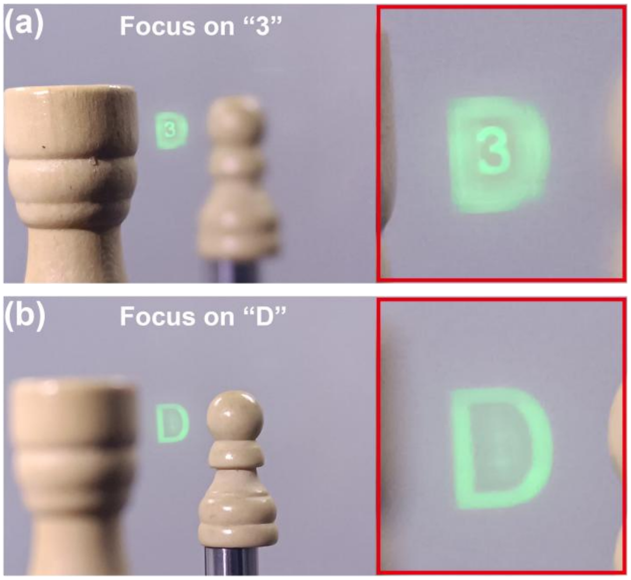

Figure 4. Reconstructed 3D images of II-based NED with nano-imprint metalens array in AR mode. (a) Captured image when eye focus on the plane of number "3" and chess piece "Rook". The right with red frame is the partial enlarged detail. (b) Captured image when eye focus on the plane of letter "D" and chess piece "Pawn".

3.2 Depth effect in VR mode

We also observe the depth effect in VR mode, as shown in figure 5. In VR mode, the image results look pretty much the same as in AR mode, but the environment is changed to a dark black background . On the reconstructed depth plane of number "3", as shown in figure 5 (a), number 3 can be clearly seen, while the peripheral letter "D" is not fully reconstructed, still fuzzy and not sharp. On the contrary, on the reconstructed depth plane of letter "D", as shown in figure 5(b), letter "D" is reconstructed clearly, while the number "3" in the middle has been far away from its reconstructed depth plane and cannot be mapped. Therefore, the depth effect has been obviously observed in the VR experiment.

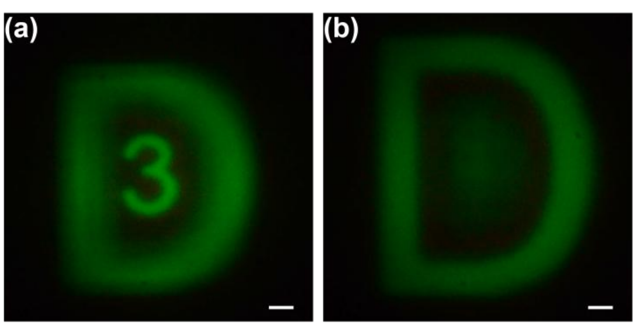

Figure 5. Reconstructed 3D images of II-based NED with nano-imprint metalens array in VR mode. (a) Captured image when eye focus on the number "3". (b) Captured image when eye focus on the letter "D".

3.3 Parallax effect in II dispaly

Subsequently, we fulfill the parallax experiments on the real mode of II display. Consider a simple situation to verify the parallax effect: the number "3", the letter "A" and "B" are located at the same central depth plane (36 mm in this system, called Plane "A3B"), and the letter "D" is 10 mm behind it, as shown in figure 6(a). The distance between the metalens array and the film source is about 5 mm. Figure 6(b-d) are the experimental images at the view angles of -1º, 0º and 1º respectively, anchoring the position of the receiving surface on Plane "A3B". Since the number "3" is reconstructed on the captured surface but the letter "D" is in front, one can see that the number "3" is always clear and sharp at all view angles while the letter "D" is relatively fuzzy. When the view angle is 0°, as shown in figure 6(c), the location of number "3" is right in the middle of the letter "D". At the same time, the letters "A" and "B" cannot be fully read because they are restricted by the field of view. However, number "3" is close to the line of the letter "D" at -1º in figure 6(b), and the letter "A" can be read more clearly. At the view angle of 1º in figure 6(d), number "3" approaches the arc part of letter "D", and the letter "B" emerges brightly. The images at different view angles have evident differences, demonstrating that parallax plays a good role in such II display. Hence, the parallax effect has been proved obviously.

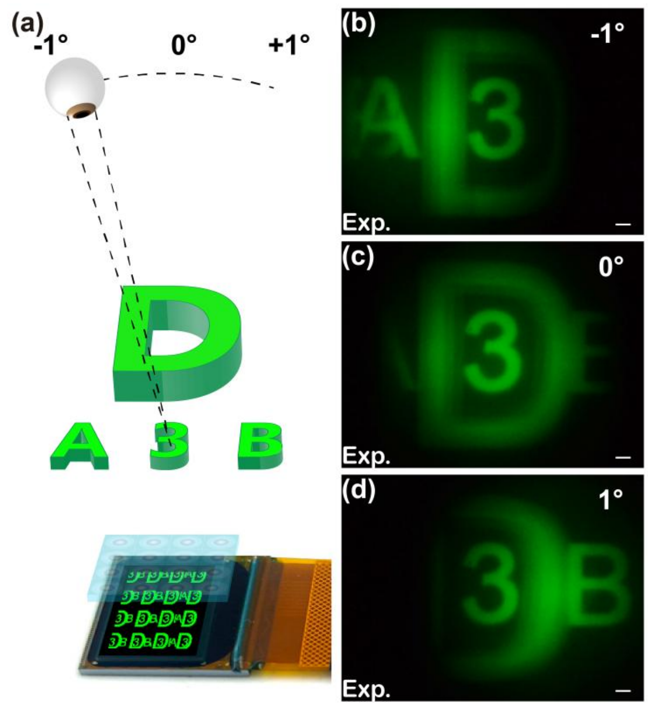

Figure 6. Reconstructed 3D parallax image of II display with nano-imprint metalens array. (a) Optical path diagrams for the 3D parallax effect in II display. (b-d) Captured images at the view angle of -1º, 0º and 1º respectively.

4. Discussions and Conclusions

In conclusions, we propose a novel II-based NED combined with metalens array. We miniaturize such II-based NED architecture by using the 3D printed holder to assemble the micro-display and the nano-imprinting metalens array. Finally, we show the effect of depth of field in both AR and VR mode and the effect of 3D real image parallax of II display. It is expected that metalens array with the ability of multi-dimensional light control can further improve the performance of II-based NED in the future. This work verifies the feasibility of nanoimprint technology for mass preparation of metalens samples, and we expect that this II-based NED system using the metalens array can be applied in the fields of VR/AR and 3D display.

5. Acknowledgements
This work is supported by Natural Science Foundation of Guangdong Province (Grant No. 2023B1515040023)， National Key R&D Program of China (Grant No.2021YFB2802300), National Key R&D Program of China (Grant No.2022YFB3602803), National Natural Science Foundation of China (Grant No. 62035016), Natural Science Foundation of Guangdong Province (Grant No.2021A1515011449), China Postdoctoral Science Foundation (Grant No.2021M703666), Guangdong Basic and Applied Basic Research Foundation (Grant No.2020A1515110661)

6. References
[1] F. L. Kooi & A. Toet. "Visual comfort of binocular and 3D displays," Displays 25, 99-108 (2004).

[2] H. Hiura, K. Komine, J. Arai & T. Mishina. "Measurement of static convergence and accommodation responses to images of integral photography and binocular stereoscopy," Opt. Express 25, 3454-3468 (2017).

[3] J. Geng. "Three-dimensional display technologies," Adv. Opt. Photon. 5, 456-535 (2013).

[4] G. Lippmann. "La photographie intégrale," C.R. Hebd. Seances Acad. Sci. 146, 446-451 (1908).

[5] Q.-H. Wang, C.-C. Ji, L. Li & H. Deng. "Dual-view integral imaging 3D display by using orthogonal polarizer array and polarization switcher," Opt. Express 24, 9-16 (2016).

[6] H. Choi, S.-W. Min, S. Jung, J.-H. Park & B. Lee. "Multiple-viewing-zone integral imaging using a dynamic barrier array for three-dimensional displays," Opt. Express 11, 927-932 (2003).

[7] S. Yang et al. "162-inch 3D light field display based on aspheric lens array and holographic functional screen," Opt. Express 26, 33013-33021 (2018).

[8] Z.-B. Fan et al. "A broadband achromatic metalens array for integral imaging in the visible," Light: Science & Applications 8, 67 (2019).

[9] D. Lanman & D. Luebke. "Near-eye light field displays," ACM Transactions on Graphics (TOG) 32, 1-10 (2013).

[10] H. Huang & H. Hua. "High-performance integral-imaging-based light field augmented reality display using freeform optics," Opt. Express 26, 17578-17590 (2018).

[11] H. Huang & H. Hua. "An integral-imaging-based head-mounted light field display using a tunable lens and aperture array," Journal of the Society for Information Display 25, 200-207 (2017).

[12] H. Li, S. Wang, Y. Zhao, J. Wei & M. Piao. "Large-scale elemental image array generation in integral imaging based on scale invariant feature transform and discrete viewpoint acquisition," Displays 69, 102025 (2021).

[13] J.-S. Park et al. "All-Glass, Large Metalens at Visible Wavelength Using Deep-Ultraviolet Projection Lithography," Nano Letters 19, 8673-8682 (2019).

[14] T. Hu et al. "CMOS-compatible a-Si metalenses on a 12-inch glass wafer for fingerprint imaging," Nanophotonics 9, 823-830 (2020).

[15] G. Brière et al. "An Etching-Free Approach Toward Large-Scale Light-Emitting Metasurfaces," Advanced Optical Materials 7, 1801271 (2019).

[16] G. Yoon, K. Kim, D. Huh, H. Lee & J. Rho. "Single-step manufacturing of hierarchical dielectric metalens in the visible," Nature Communications 11, 2268 (2020).

[17] G.-Y. Lee et al. "Metasurface eyepiece for augmented reality," Nature Communications 9, 4562 (2018).

[18] E. Bayati, A. Wolfram, S. Colburn, L. Huang & A. Majumdar. "Design of achromatic augmented reality visors based on composite metasurfaces," Appl. Opt. 60, 844-850 (2021).

[19] Z. Li et al. "Meta-optics achieves RGB-achromatic focusing for virtual reality," Science Advances 7, eabe4458 (2021).

[20] D. K. Nikolov et al. "Metaform optics: Bridging nanophotonics and freeform optics," Science Advances 7, eabe5112 (2021).

[21] C. Wang et al. Metalens Eyepiece for 3D Holographic Near-Eye Display. Nanomaterials 11 (2021).

[22] Y. Li et al. "Ultracompact multifunctional metalens visor for augmented reality displays," PhotoniX 3, 29 (2022).

[23] Z. Li et al. "Inverse design enables large-scale high-performance meta-optics reshaping virtual reality," Nature Communications 13, 2409 (2022).